



## Fatigue Improvement of Cast Aluminum Composites via Experimental and ANSYS Analysis

Awatif Mustafa Ali<sup>\*</sup>, Adil Abed Nayeeif<sup>ID</sup>

Department of Mechanical Engineering, College of Engineering, Mustansiriyah University, Baghdad 10052, Iraq

Corresponding Author Email: [Awataf@uomustansiriyah.edu.iq](mailto:Awataf@uomustansiriyah.edu.iq)

Copyright: ©2025 The authors. This article is published by IIETA and is licensed under the CC BY 4.0 license (<http://creativecommons.org/licenses/by/4.0/>).

<https://doi.org/10.18280/rcma.350304>

### ABSTRACT

**Received:** 5 May 2025

**Revised:** 6 June 2025

**Accepted:** 18 June 2025

**Available online:** 30 June 2025

#### Keywords:

*composite aluminum alloys, fatigue test, constant loading, ZrO<sub>2</sub>, TiO<sub>2</sub> and Al<sub>2</sub>O<sub>3</sub> nanoparticles, metal matrix, tensile test, experimental, numerical (ANSYS)*

In this work, ANSYS Workbench finite element analysis and experimental testing were employed to investigate how adding ceramic reinforcements—silicon carbide (SiC) and zirconium oxide (ZrO<sub>2</sub>)—specifically enhance fatigue performance in cast aluminum matrix composites. Specimens containing 5% and 10% weight fractions of each reinforcement, prepared using sand casting, were then tested according to the ASTM A370-11 and ASTM E8/E8M standards to assess their mechanical behavior and failure characteristics. The results reveal that adding 5% SiC increases fatigue resistance, with the highest fatigue limit of any studied sample. Conversely, a 10% ZrO<sub>2</sub> content decreases fatigue performance because of internal stress concentrations and particle agglomeration. With a stress ratio of  $R = -1$  and based on the stress-life (S-N) approach, the numerical simulations produced results highly consistent with experimental data, varying from 5.2% to 8.3%. According to the study's findings, the fatigue behavior of aluminum composites is influenced by the type and concentration of reinforcing particles. SiC at 5% provides the best fatigue enhancement, whereas higher percentages—especially ZrO<sub>2</sub>—may compromise mechanical integrity. Its usefulness in the design and analysis of composite materials is supported. The finite element methods demonstrated the ability to forecast fatigue life.

## 1. INTRODUCTION

Metal-matrix composites (MMCs) have been utilized increasingly in various industries due to their enhanced properties compared to non-reinforced alloys. Among the different types of MMCs, aluminum-based composites were discovered in many applications like vehicles, drive shafts, automotive pistons, and bicycle frames. Aluminum oxide (Al<sub>2</sub>O<sub>3</sub>) and silicon carbide (SiC) particles were typically used to reinforce aluminum alloys due to their high hardness. However, the full potential of these MMCs has been limited by their high machining costs. Alumina and silicon carbide are the reinforcements most frequently investigated and used in the production of composite materials, typically in the form of short or long fibers and particles. Compared to their parent metals, ceramic particles are multiphase solid materials that demonstrate "greater specific strength, modulus of elasticity, fatigue performance, damping, and corrosion resistance [1].

Zirconium oxide (ZrO<sub>2</sub>) and silicon carbide (SiC) were chosen as reinforcement materials for their excellent mechanical and thermal qualities. Silicon carbide improves fatigue strength and wear resistance because of its high hardness, low density, and superior thermal conductivity. In contrast, zirconium oxide has excellent thermal shock resistance and fracture toughness, which are especially useful under cyclic loading circumstances. ZrO<sub>2</sub> and SiC outperform traditional reinforcements like Al<sub>2</sub>O<sub>3</sub> and TiO<sub>2</sub> by offering a

better mix of stiffness and toughness. As a result, they are ideal for reinforcing aluminum matrices in engineering applications requiring fatigue resistance. Reinforced particles are employed depending on the required properties of end products, like tensile strength, modulus, wear resistance, or to boost the dielectric permittivity of materials. Various additive manufacturing processes are employed to fabricate the composites [2].

SiC and ZrO<sub>2</sub>-reinforced aluminum composites are suitable for high-performance applications requiring fatigue resistance, thermal stability, and structural reliability. In aerospace and automotive systems, SiC improves wear resistance and stiffness, which is critical for rotating and load-bearing components subjected to repeated stress and high temperatures. ZrO<sub>2</sub>'s toughness and thermal shock resistance make it ideal for thermal barrier coatings, heat exchangers, and electronics enclosures. These applications necessitate careful control over microstructure, interfacial bonding, and reinforcement distribution to assure durability and performance under demanding service conditions.

## 2. LITERATURE REVIEW

Recent decades have seen a surge in global research on metal matrix composites reinforced with particles, with a particular focus on the addition method during the

manufacturing process [3]. Liu et al. [4] prepared TiB<sub>2</sub>/2024 aluminum matrix composite in situ and compared it with 2024-T4 aluminum alloy (2024Al). Stress-strain-controlled fatigue experiments were conducted to obtain the fatigue life. The outcome is that adding in-situ particles enhances fatigue resistance. Al 6061, another type of aluminum to improve its physical properties reinforced by Al<sub>2</sub>O<sub>3</sub> with 40, 60 & 100 µm in grain size and the weight ratio of 0-16 wt% was studied by Mahendra et al. [5]. A significant improvement in fatigue and fracture toughness properties was observed [5]. To gain a deeper understanding of the effect of stress concentration caused by the state of machined surfaces on fatigue behavior, Xiong et al. [6] investigated the fatigue performance of machined in-situ TiB<sub>2</sub>/7050Al metal matrix composite (MMC) specimens. They thoroughly examined fatigue mechanisms, stress concentration, fatigue life, and life modelling. Their findings revealed that the fatigue life ranged from  $1.0 \times 10^5$  to  $4.0 \times 10^6$  cycles, indicating a significant instance of high-cycle fatigue. Additionally, as surface roughness increased, fatigue life decreased sharply. Adding another element like Zr and investigating the effects of TiB<sub>2</sub> and Zr on the microstructure and mechanical properties of heat-extruded Al–Zn–Mg–Cu-based materials. Results showed that TiB<sub>2</sub> increased grain size during solidification, while zircon had a minimal effect on grain improvement but suppressed recrystallisation and grain growth. TiB<sub>2</sub> enhanced ageing kinetics and peak hardness, whereas zircon improved peak hardness with little impact on ageing. Additionally, quenching sensitivity, elastic modulus, and tensile properties were compared [7]. Casting and alloying methods significantly affect the properties of alloys. In Ji-dong Zhang's study, zirconium oxide-enhanced 7075 aluminum was produced successfully using spark plasma sintering (SPS). The research also showed that adding zirconium oxide increased but later decreased the density, hardness, ultimate tensile strength, and elongation [8]. Others examined the potential of Aluminum Metal Matrix Composites (AMMCs) as an alternative to conventional steel bars, emphasizing sustainability and performance. The research shows that AMMCs have a yield stress of 869 MPa, surpassing the 600 MPa requirement for Fe600 bars, and an elongation percentage of 40.87%, meeting IS: 1786–2008 guidelines. Additionally, they demonstrate a Young's Modulus value exceeding 200 GPa, in line with IS: 456–2000 standards. These findings suggest that AMMCs can effectively replace steel bars in reinforced concrete elements while supporting a sustainable construction future, reducing carbon footprints, and adhering to environmental regulations [9]. Wang and Monetta [10] studied the preparation process, microstructure, mechanical characteristics, wear resistance, and applications of SiC particle-reinforced metal matrix composites (MMCs). It examines how interfacial reactions impact the macroscopic characteristics of the materials and emphasizes the connection between mechanical and microstructure characteristics. Along with outlining possible future development routes, the report also provides an overview of the applications of these composites in the electronics, automotive, and aerospace industries. The results offer a useful guide for future studies and uses of SiC particle-reinforced MMCs [10]. Creating permanent hybrid materials by directly joining dissimilar metals presents a significant engineering challenge due to the substantial metallurgical difficulties associated with their extreme differences [11]. Research has demonstrated that many scholars have successfully synthesized high-

performance products [12, 13]. Tensile testing and scanning electron microscopy were used to examine the microstructure and mechanical characteristics of SiC/Al composites. The findings demonstrated that the homogeneity of the SiC particle dispersion has a substantial impact on the mechanical properties [14, 15]. For automotive components made using the stir casting method, the researcher prepared composites of 7075 aluminum alloy reinforced with zirconium dioxide (ZrO<sub>2</sub>). Microscopic analysis showed improved dispersion of reinforcements along grain boundaries, resulting in an improved structure. The composite containing 6% ZrO<sub>2</sub> showed enhanced performance associated with this grain improvement [16]. The construction industry increasingly utilizes aluminum alloys because of their advantageous properties. This trend has led to extensive research aimed at gaining a better understanding of the structural behavior of these alloys, as well as the creation of accurate and reliable design principles [17]. High-strength aluminum alloys used in transportation structures have poor fatigue performance, requiring engineers to design around this limitation for lightweight applications. A new microstructure design improves fatigue strength by utilizing the mechanical energy from initial fatigue cycles to heal weak points in the microstructure. This approach increases the fatigue life of the highest-strength aluminum alloys by 25 times and fatigue strength to about half of the tensile strength, marking a shift in microstructural design focused on fatigue performance [18]. A finite element simulation was used to forecast the fatigue life of Al 2024-T351 under uniaxial loads at both room temperature and higher temperatures. Using an MTS 810 servo-hydraulic machine with an MTS 653 high-temperature furnace, monotonic tensile and cyclic tests were performed at 100°C and 200°C with a frequency of 10 Hz and a load ratio of 0.1. Yield strength rose by 8% and ultimate strength by 2.32 MPa at 100°C. In comparison to room temperature, yield strength varied marginally (1.61 MPa) while ultimate strength decreased by 25% at 200°C. High temperatures decreased fatigue life by hastening the beginning and spread of cracks. When mechanical characteristics and fatigue data were entered into ANSYS, the simulation's output closely matched the experimental findings [19]. A numerical investigation to estimate the fatigue life of a cylindrical aluminum alloy specimen under high cycle fatigue conditions. The stress-life approach is used to evaluate the fatigue life. Either an equivalent defect or a collection of surface flaws damages the sample. There are two types of flaws: session load conditions with a load ratio  $R = 0.1$  are postulated. The Goodman adjustment is applied to account for non-zero mean stress. Using ANSYS Workbench software, the material properties are regarded as a combination of nonlinear isotropic and kinematic hardening [20]. The fatigue life, fatigue strength, and safety parameters for as-cast AA5052 and its composites, AA5052/7 weight per percent ZrO<sub>2</sub>, TiO<sub>2</sub>, and Al<sub>2</sub>O<sub>3</sub>, were successfully predicted using the finite element method using ANSYS Workbench 16. 1. 504 elements and 2572 nodes were included in the FEA model, which was based on the size of the experimental specimen. Using the Goodman theory, fatigue analysis was carried out in static structural circumstances. The fatigue life variations for the ZrO<sub>2</sub> composite ranged from 1.4% to 17%, which was in close agreement with simulation results and experimental data. The Al<sub>2</sub>O<sub>3</sub> composite had the lowest average error of 0.378%, while the highest was 2.031% (AA5052). Differences in fatigue strength at 10<sup>7</sup> cycles were less for the composites and within 4.14% for the matrix. For

AA5052, the minimum safety factor was 0.8327, while for the composites, it was approximately 1.070 [21].

This study investigates the enhancement of fatigue resistance in cast aluminum composites through experimental methods and numerical analysis using ANSYS software. Composite samples were fabricated using a casting process, incorporating SiC and ZrO<sub>2</sub> reinforcement to improve mechanical properties. Tensile and fatigue tests were conducted to evaluate the mechanical behavior and identify the failure mechanisms under cyclic loading. Based on the findings, it is clear that reinforcement content is crucial in determining the mechanical behavior of aluminum matrix composites. Advised is to add in small amounts and at a very fine grain size to get the best results.

### 3. MATERIALS AND METHODS

#### 3.1 Materials

Aluminum is the metal employed in this study. Table 1 shows the result of a chemical analysis we performed at the General Institution for Rehabilitation and Engineering Inspection.

**Table 1.** Chemical composition of the alloys

AL	Cu	Zn	Ni	Fe	Mn
Base	5.0	0.011	0.15	0.38	0.19

Zirconium oxide, sometimes known as "ceramic steel", is thought to be one of the most promising materials for restorative applications due to its remarkable mechanical properties. It has no chemical properties, resistance to expansion at high temperatures, chemical resistance, low heat conductivity, and strong mechanical resistance [22].

The basic semiconductor material, silicon carbide, or SiC, was created by combining pure silicon and pure carbon. When feeding the material, silicon carbide 88 lump has no dust nuisance, good thermal conductivity, consistent chemical characteristics, and the capacity to remove oxygen and modify carbon content [23]. The reinforcement is shown in Figure 1.



**Figure 1.** Reinforcement additive

#### 3.2 Methods

The sand mould was used. The sand was first sieved, then moistened with water, pressed tightly to hold it together, and finally compacted. After the placement of the anchoring pipes, the stickiness increased further due to compaction, as illustrated in Figure 2.

After being deposited in a crucible, the aluminum is melted in a furnace at temperatures higher than 660°C. To achieve

precise temperature monitoring, a thermocouple is interfaced with a PID controller before being poured into a heated mould (at 200°C). As depicted in Figure 3.



**Figure 2.** Sand casting equipment (a) Sieves and (b) Cast mold



**Figure 3.** Metal melting

Zirconium oxide and silicon carbide addition ratios are prepared using the weight ratio method and then wrapped in aluminum foil. To minimize thermal gradients and moisture discrepancies, the reinforcement particles (SiC or ZrO<sub>2</sub>) are preheated to about 300°C using a separate furnace and progressively introduced to the molten aluminum. An electric mixer was then used to agitate for 10 minutes, according to Figure 4(a), to obtain samples containing the proper additives in materials and ratios (5% and 10%) from SiC and ZrO<sub>2</sub>, and repeat the previous procedure.

Finally, extract the sample, remove any surplus metal, and perform an initial cleaning as illustrated in Figure 4(b).

Following casting, the composite samples were first cleaned to eliminate any extra material or surface imperfections, and the specimens were then cut on a precision lathe to the standard geometries necessary for tensile and fatigue testing. The dimensions were meticulously checked in line with ASTM A370-11 and ASTM E8/E8M standards to ensure uniformity and comparability across all samples. Proper alignment and surface finish were maintained throughout turning to avoid introducing stress concentrators that could impair mechanical performance.

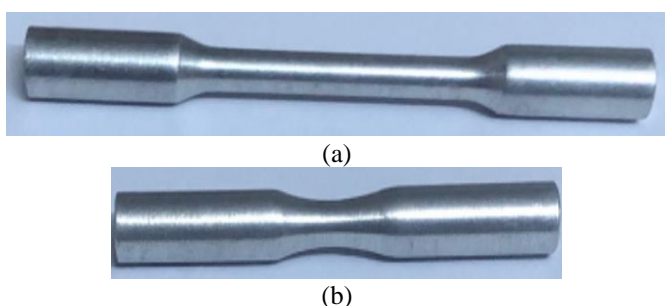
Tensile testing was conducted using specimens that were accurately machined to defined geometries and dimensions in compliance with ASTM A370-11 [24] to guarantee accurate and consistent findings. For precise tensile strength measurements, this level of sample preparation precision was essential. Fatigue testing was conducted according to ASTM E8/E8M [25], as depicted in Figure 5, which also shows the testing equipment in Figure 6 and the produced specimens.





(a) Electronic compact scale (b) Extract the sample

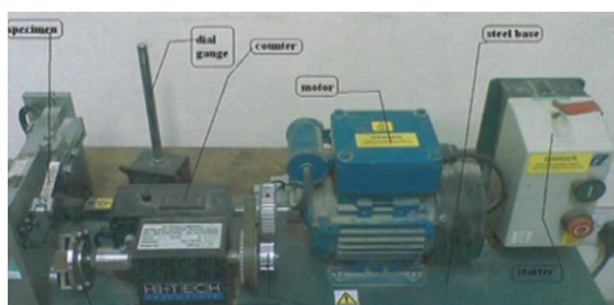
**Figure 4.** Sample preparation and weighing for laboratory testing



(a)

(b)

**Figure 5.** Standard specimens for (a) Tensile and (b) Fatigue testing



(a)



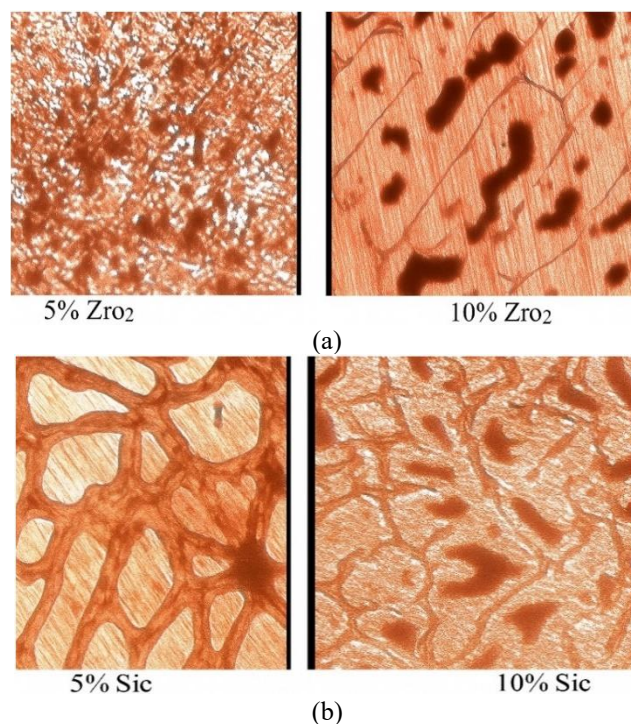
(b)

**Figure 6.** Standard devices for (a) Fatigue and (b) Tensile testing

## 4. RESULTS AND DISCUSSIONS

### 4.1 Microstructural characterization

The properties of the metal used are presented in Table 1, whereas the following Figures 7(a) and (b) illustrate its microstructure. The microscope used in the test is a beam engineer's RMM-7T 2003 (1200x). With 5%  $ZrO_2$ , the microstructure is uniform with small, evenly distributed grains and no visible pores or cracks. It indicates a dense structure with excellent mechanical strength and fracture resistance. While 10%  $ZrO_2$ , the sample has large pores and larger grains with visible lines, suggesting grain growth or phase boundaries. So, the increase in  $ZrO_2$  to 10% leads to porosity, which may negatively impact toughness and hardness.



5%  $ZrO_2$

10%  $ZrO_2$

5% SiC

10% SiC

**Figure 7.** Microstructure for the two types

### 4.2 Experimental result

Aluminum matrix composites are meticulously engineered materials that blend the toughness of the aluminum alloy matrix with the exceptional hardness, stiffness, and strength provided by rigid reinforcements, such as silicon carbide (SiC) and zirconia ( $ZrO_2$ ). This innovative combination results in a composite material that offers an impressive synergy of strength and toughness, making it suitable for different demanding applications.

The interaction between the matrix and the reinforcements creates elastic and plastic incompatibilities, leading to the development of interaction stresses. These stresses play a crucial role in the overall performance of the material. The unique complex phases of SiC and  $ZrO_2$  actively contribute to the stability of the composite by safeguarding against grain boundary sliding. This protective mechanism hinders the easy flow of material, thereby enhancing the structural integrity of the composite.

Research findings on strain measurements reveal a notable increase in strain values as the proportion of SiC reinforcement rises between 5% and 10%. Conversely, the addition of  $ZrO_2$

results in a decrease in strain values when compared to SiC, highlighting the differing effects of these reinforcements on material behaviour. Similarly, ultimate stress measurements indicate a significant increase in strength with higher quantities of ZrO<sub>2</sub> (5%-10%), while the strain responses again show a reduction with SiC. This nuanced understanding of the interplay between the different reinforcements underscores the potential of aluminum matrix composites in a wide array of engineering applications, as shown in Figure 8.

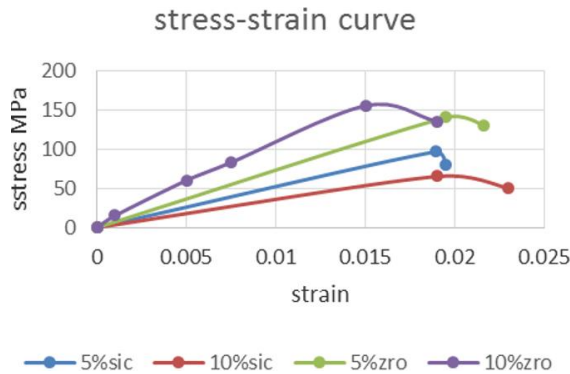


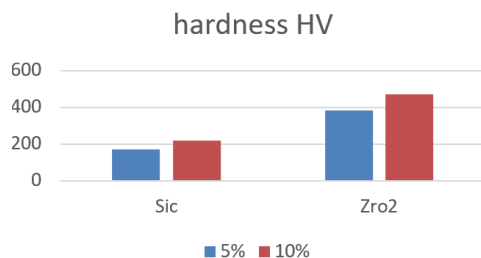
**Figure 8.** Stress-strain curve

The hardness data show that increasing the ceramic reinforcing content increases the material's resistance to deformation. The 10% ZrO<sub>2</sub> sample exhibited the highest hardness (470 HV), followed by the 5% ZrO<sub>2</sub> sample (383.7 HV). SiC-reinforced samples had lower hardness values (220 HV for 10% and 171.4 HV for 5%). This trend highlights the hardness of ZrO<sub>2</sub> and the impact of greater reinforcing content. However, excessive reinforcement can cause brittleness and internal flaws, reducing fatigue performance despite increased hardness, as shown in Table 2.

**Table 2.** Hardness values for aluminum composites enhanced with SiC and ZrO<sub>2</sub>

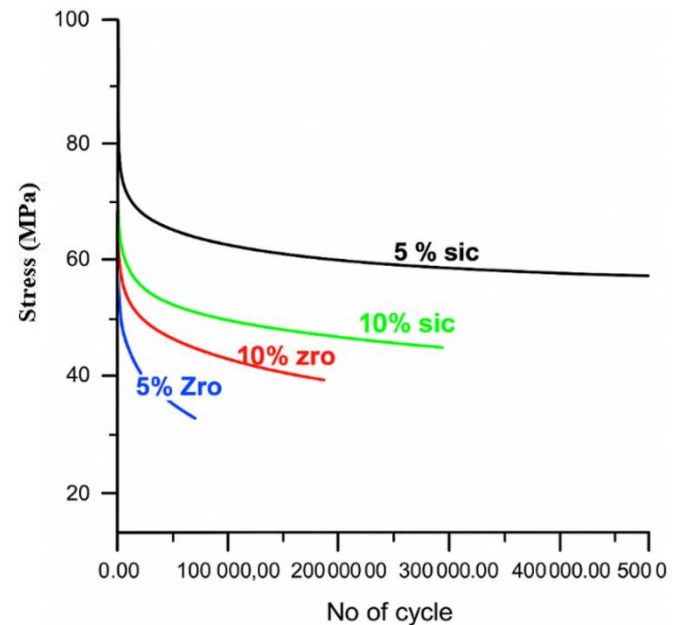
Type	(HV)	B (HB)	D (mm)	F (N)	T (sec)
5% ZrO <sub>2</sub>	383.7	364.7	31.09	1.962	10
5% SiC	171.4	163.1	46.51	1.962	10
10% ZrO <sub>2</sub>	470	440	28.0	1.962	10
10% SiC	220	230	40.0	1.962	10

Figure 9 shows the Vickers hardness (HV) values for SiC and ZrO<sub>2</sub> at two concentrations (5% and 10%). The hardness of both materials increases with increasing concentration. ZrO<sub>2</sub> has much higher hardness than SiC at both levels, with the greatest value measured at 10%. ZrO<sub>2</sub> has superior mechanical qualities and microstructural characteristics that improve resistance at larger concentrations, making it more effective in increasing hardness.



**Figure 9.** Vickers hardness (HV) for SiC and ZrO<sub>2</sub> at 5% and 10% concentrations

The maximum number of cycles under dynamic load is 500000 for the 5% silicon carbide (SiC) alloy. This improvement is due to the uniform distribution of particles (SiC and ZrO<sub>2</sub>) within the alloy, which exhibits lower porosity. The enhancement of the composite properties is affected by several factors: the intrinsic properties of both the reinforcement and the matrix, the uniformity of the reinforcement distribution, its particle size and volume ratio, and the bond strength at the interface between these constituents. All of these factors play a crucial role in determining the mechanical properties of the composite, as shown in Figure 10.



**Figure 10.** The stress applied with the number of cycles to all alloys

### 4.3 Numerical results

In the current investigation, fatigue life and strength with various parameter effects were calculated numerically using the finite element method (FEM) with the use of ANSYS software tools [20]. Building the geometry and choosing the element type are the initial steps in analyzing the fatigue problem for the materials needed. This paper analyses the application of stress, creep, significant deflection, and strain using a solid (187) element type, which is regarded as a 3-D higher order with 10 nodes. Then, the analysis required meshing the molding for the fatigue sample by using the mesh generation technique to calculate the best mesh size. The final step is to apply the boundary conditions similar to the experimental work and conduct a stress-life approach to the fatigue test using the stress ratio  $R=-1$ .

The simulation's finite element mesh is depicted in Figure 11, without any outcome contours. A central notch in the double-cone form of the model geometry simulates a zone of stress concentration. Accurately recording the stress distribution requires a high density of triangular elements in the mesh, particularly focused near the notch area. This area's mesh refinement makes sure that local stress variations are accurately represented, which improves the fatigue analysis's accuracy. For finite element analysis to produce accurate fatigue life predictions, this mesh configuration is necessary.

The findings of a fatigue life study carried out in ANSYS

2019 are shown in Figure 12. The model represents a notched specimen under cyclic loading. With values ranging from blue to red, the color contour shows the number of cycles before failure. The red-highlighted notch region in the middle of the specimen shows the highest concentration of stress and, hence, the lowest fatigue life. The result suggests that under repeated loading circumstances, the specimen is most likely to fail at this site. To better capture stress gradients, the mesh's triangular components are refined close to the notch area.

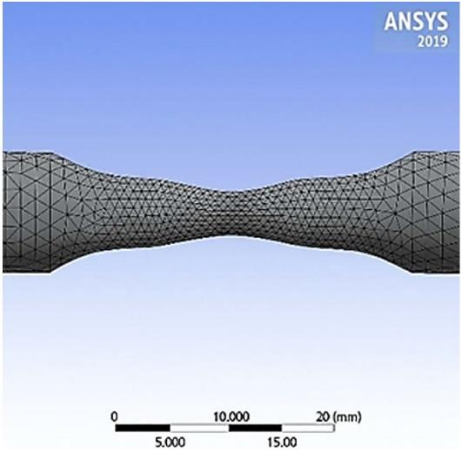


**Figure 11.** Mesh of the notched geometry with finite elements

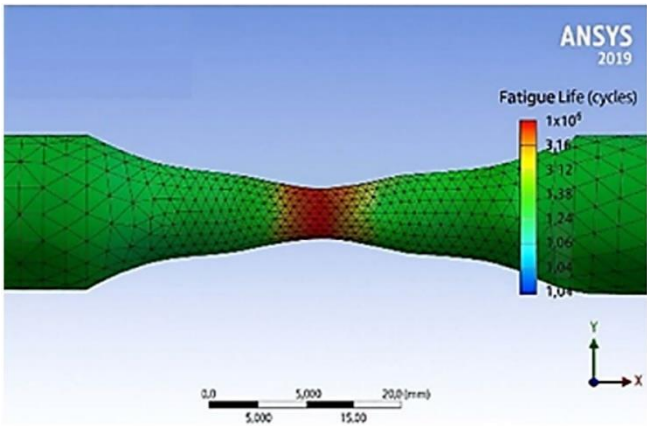


**Figure 12.** Distribution of fatigue life

Comparing experimental and numerical results, the presented S-N curves show the fatigue performance of composite materials reinforced with 5% SiC, 5% ZrO<sub>2</sub>, and 10% ZrO<sub>2</sub>. These charts show the usual fatigue behavior of metallic and composite materials, where the alternating stress needed for failure reduces as the number of cycles increases. The curves also provide information about how well numerical forecasts work and how reinforcement content affects fatigue life.

Figures 13 to 16 show the theoretical and scientific stress and fatigue life curves for four samples of composite materials at 5% and 10% for each silica carbide and zirconium oxide. We note that the results of the specific elements are less than the results of the practical test according to the percentage of each sample.

For 5% SiC-reinforced material, the experimental and numerical S-N curves are shown in Figure 12. Stress and life typically have an inverse relationship. Although the numerical results often underestimate the fatigue life by a small amount

at each stress level, they roughly match the experimental pattern. Fatigue models based on finite elements frequently exhibit this conservative forecast due to assumed boundary conditions and simplifications.

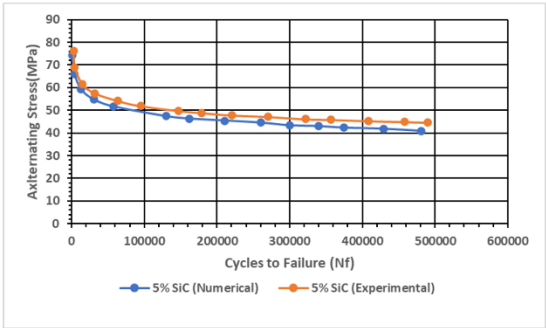


**Figure 13.** Experimental and numerical fatigue life comparison for 5% SiC

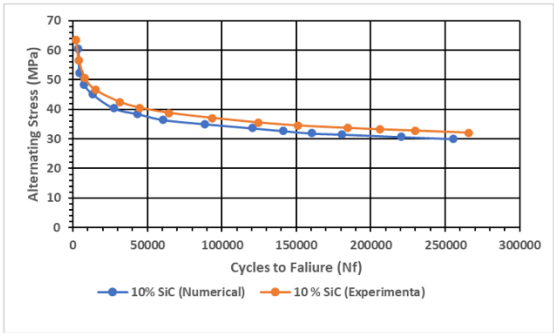


**Figure14.** Experimental and numerical fatigue life comparison for 10% SiC

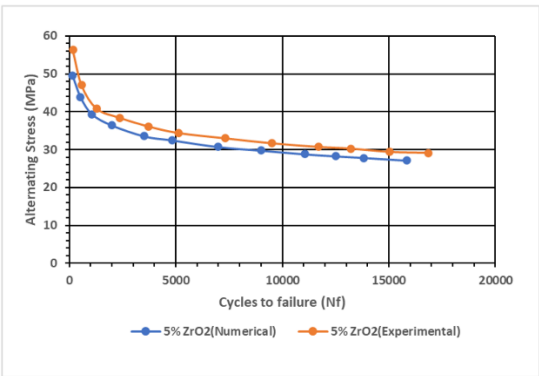


**Figure 15.** Experimental and numerical fatigue life comparison for 5% ZrO<sub>2</sub>

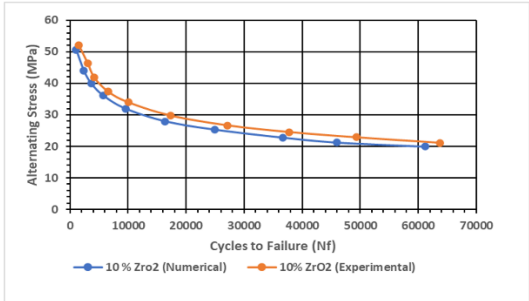


**Figure 16.** Experimental and numerical fatigue life comparison for 10% ZrO<sub>2</sub>

A gradual slope in the experimental data indicates excellent



fatigue resistance. SiC particles boost fatigue strength by stopping cracks from starting and spreading through how loads are transferred and by changing the direction of cracks.

In comparison to 5% ZrO<sub>2</sub>, the 10% ZrO<sub>2</sub> composite exhibits a steeper stress fall with increasing cycles and noticeably lower stress levels in the S-N curve. This suggests that increasing the reinforcement content may lead to a trade-off in performance. As the stiffness and hardness increase, too many ZrO<sub>2</sub> particles could aggregate, causing internal stress raisers and microstructural irregularities that lead to early fatigue cracks. Once more, numerical predictions demonstrate the resilience of the employed modelling technique by following the experimental data with a respectable degree of precision.

The 5% SiC-reinforced composite's balanced mechanical reinforcement and dispersion give it exceptional fatigue resistance. While ZrO<sub>2</sub> offers similar advantages at 5%, its performance degrades at 10% as a result of embrittlement and crack-promoting properties.

The experimental and numerical fatigue life equations and fatigue limits for various composite samples are compared in Table 3. With variations ranging from 5.20% to 8.27%, the data show a consistent pattern where the experimental fatigue limits are somewhat higher than the numerical predictions. This deviation falls within allowable bounds for fatigue modelling, demonstrating the numerical simulation's dependability and conservatism. Sample 1, which is probably reinforced with 5% SiC, has the highest fatigue limit (51.545 MPa), which is consistent with its improved fatigue performance as seen by the S-N curves. Sample 4, on the other hand, shows the lowest fatigue limit (19.527 MPa), most likely as a result of either a higher reinforcing content or distinct loading circumstances that worsen stress concentrations and crack initiation.

**Table 3.** Experimental and numerical fatigue limit for different composite samples

No.	Fatigue Life Equation		Fatigue Limit (MPa)		Deviations %
	Exp.	Numer.	Exp.	Numer.	
1	$\sigma_L = 150.38 N_f^{-0.093}$	$\sigma_L = 158.12 N_f^{-0.102}$	51.545	48.863	5.203
2	$\sigma_L = 161.97 N_f^{-0.13}$	$\sigma_L = 157.6 N_f^{-0.133}$	36.260	34.084	6.001
3	$\sigma_L = 150.34 N_f^{-0.135}$	$\sigma_L = 129.67 N_f^{-0.128}$	31.774	29.705	6.511
4	$\sigma_L = 313.07 N_f^{-0.241}$	$\sigma_L = 293.88 N_f^{-0.243}$	19.527	17.913	8.265

Finite element simulations using ANSYS Workbench provided a full understanding of fatigue behavior in aluminum matrix composites that are cast and augmented with SiC and ZrO<sub>2</sub>. The stress-life (S-N) fatigue method, which involves applying a fully reversed load ( $R = -1$ ), showed that the simulations matched the experimental results closely, with differences between 5.2% and 8.3%.

The modelling of the 5% SiC-reinforced composite showed a delay in fracture development due to enhanced stiffness and load transfer efficiency. The uniform dispersion of SiC particles reduces localized stress peaks, resulting in a longer fatigue life. However, as the reinforcement content rises to

10%, particle clumping and poor wettability introduce stressors, limiting effective fatigue resistance. The 10% ZrO<sub>2</sub> samples showed a decrease in performance, as demonstrated by both simulation and experimental evidence. ZrO<sub>2</sub> particles' high density and inclination to form agglomerates resulted in non-uniform stress fields, leading to early failure.

The ANSYS model is accurate because it closely replicates the physical test setup and assigns boundary conditions, material properties, and loading profiles correctly. However, there are still some limitations, like the model's difficulty in accurately showing small defects such as holes or weak spots between materials. Nonetheless, the simulation's cautious estimates serve as a realistic benchmark for designing composite structures and assessing their fatigue life. The remarkable connection with experimental results indicates the numerical model's stability when properly calibrated.

From Sample 1 to Sample 4, the fatigue life exponents (b-values) show more negative values, indicating a larger decrease in fatigue strength with more cycles, especially in materials that are more brittle or reinforced. Overall, the table confirms the accuracy of the numerical method for predictive fatigue analysis in composite materials and highlights how mild reinforcing can improve fatigue resistance.

The fatigue stress values for composite samples with different amounts of ZrO<sub>2</sub> (zinc oxide) and SiC (silicon carbide) are shown in Figure 15. At roughly 52 MPa, the 10% SiC sample is found to have the highest fatigue stress, closely followed by the 10% ZrO<sub>2</sub> sample. Both SiC and ZrO<sub>2</sub> specimens have a comparable decrease in fatigue stress as the reinforcement content reduces below 5%. Interestingly, for equivalent weight percentages, SiC-reinforced composites continuously exhibit greater fatigue resistance than ZrO<sub>2</sub>. This evidence suggests that SiC particles enhance fatigue performance more successfully, most likely as a result of improved load transfer efficiency and interfacial bonding. The significance of suitable filler loading in improving fatigue properties is highlighted by the decrease in fatigue stress with reduced reinforcing content.

SiC increases fatigue life principally because of its high stiffness and crack-arresting capacity. Its homogeneous dispersion promotes stress redistribution, reduces local strain accumulation, and delays crack onset. ZrO<sub>2</sub> enhances fatigue resistance by transformation toughening, where stress-induced phase shifts generate compressive stresses at fracture tips. Excessive ZrO<sub>2</sub> causes particle aggregation, stress concentration, and early failure. Therefore, a balance of reinforcement dispersion, interfacial bonding, and the appropriate volume fraction determines fatigue performance.

## 5. CONCLUSIONS

Reinforcement particle types and proportions have a major impact on the material's fatigue behaviour. With a higher stress level maintained over a larger number of cycles, the specimen with 5% SiC showed the maximum fatigue resistance. Specimens containing 5% and 10% ZrO<sub>2</sub>, on the other hand, demonstrated poorer fatigue performance and a more pronounced stress decrease with an increase in cycles. Although it was marginally less durable than the 5% SiC sample, the 10% SiC specimen outperformed the two ZrO<sub>2</sub> samples. In this composite system, our findings imply that SiC reinforcement improves fatigue life more efficiently than ZrO<sub>2</sub>, especially at lower concentrations.

These fatigue experiments and the numerical calculations that go along with them show how important the volume percentage and kind of reinforcement are in determining fatigue performance. The best amounts of reinforcement (5% ZrO<sub>2</sub> or 5% SiC) improve fatigue resistance; however, too much ceramic (10% ZrO<sub>2</sub>) might cause microstructural problems that impair performance. For predictive analysis in composite design, the numerical models offer a consistent and conservative estimate of fatigue life.

Higher deviations (8.3% in Sample 4) may be the result of more intricate fracture propagation mechanisms or simplifications in the numerical model. Fatigue modelling deems deviations between 5.2% and 8.3% acceptable, confirming the accuracy of the numerical simulations.

This study has limitations, including the exclusive use of SiC and ZrO<sub>2</sub> particles without exploring potential synergistic effects from hybrid or nanoscale reinforcements. Fatigue behavior was assessed under constant amplitude loading (R = -1), which does not reflect variable service conditions. The numerical model assumes material homogeneity and perfect interfacial bonding, overlooking critical factors like porosity and particle agglomeration. Thermal and environmental effects that could significantly impact fatigue life were also not taken into consideration.

## ACKNOWLEDGMENT

The authors thank the Ministry of Higher Education (MOHE) and Mustansiriyah University (www.uomustansiriyah.edu.iq) for the approved funding, which makes this research viable and effective.

## REFERENCES

- [1] Su, J., Li, Y.Z., Duan, M.G., Liu, S.H., Liu, K. (2018). Investigation on particle strengthening effect in in-situ TiB<sub>2</sub>/2024 composite by nanoindentation test. *Materials Science and Engineering: A*, 727: 29-37. <https://doi.org/10.1016/j.msea.2018.04.070>
- [2] Sekar, K., Jayachandra, G., Aravindan, S. (2018). Mechanical and welding properties of A6082-SiC-ZrO<sub>2</sub> hybrid composite fabricated by stir and squeeze casting. *Materials Today: Proceedings*, 5(9): 20268-20277. <https://doi.org/10.1016/j.matpr.2018.06.398>
- [3] Pramanik, A., Islam, M.N., Davies, I.J., Boswell, B., Dong, Y., Basak, A.K., Uddin, M.S., Dixit, A.R., Chattopadhyaya, S. (2017). Contribution of machining to the fatigue behaviour of metal matrix composites (MMCs) of varying reinforcement size. *International Journal of Fatigue*, 102: 9-17. <https://doi.org/10.1016/j.ijfatigue.2017.04.018>
- [4] Liu, K., Li, Y.Z., Duan, M.G., Zhang, T., Li, C., Li, B. (2021). Fatigue life prediction of in-situ TiB<sub>2</sub>/2024 aluminum matrix composite. *International Journal of Fatigue*, 145: 106128. <https://doi.org/10.1016/j.ijfatigue.2020.106128>
- [5] Mahendra, H.M., Prakash, G.S., Prasad, K.K., Rajanna, S. (2020). Fatigue and fracture behaviour of Al6061-Al<sub>2</sub>O<sub>3</sub> metal matrix composite: Effect of heat treatment. In *IOP Conference Series: Materials Science and Engineering*, Karnataka, India, 925(1): 012042. <https://doi.org/10.1088/1757-899X/925/1/012042>
- [6] Xiong, Y.F., Wang, W.H., Shi, Y.Y., Jiang, R.S., Lin, K.Y., Liu, X.F. (2020). Fatigue behavior of in-situ TiB<sub>2</sub>/7050Al metal matrix composites: Fracture mechanisms and fatigue life modeling after milling. *International Journal of Fatigue*, 138: 105698. <https://doi.org/10.1016/j.ijfatigue.2020.105698>
- [7] Xiao, H.Y., Li, Y.G., Geng, J.W., Li, H.P., Wang, M.L., Dong, C., Li, Z.G., Wang, H.W. (2021). Effects of nano-sized TiB<sub>2</sub> particles and Al<sub>3</sub>Zr dispersoids on microstructure and mechanical properties of Al-Zn-Mg-Cu based materials. *Transactions of Nonferrous Metals Society of China*, 31(8): 2189-2207. [https://doi.org/10.1016/S1003-6326\(21\)65648-0](https://doi.org/10.1016/S1003-6326(21)65648-0)
- [8] Zhang, J.D., Zhang, L., Ma, H.Z. (2023). Effect of ZrO<sub>2</sub> additions on the microstructure, mechanical and wear properties of ZrO<sub>2</sub>/7075 aluminium alloy composite. *Materials Today Communications*, 37: 107437. <https://doi.org/10.1016/j.mtcomm.2023.107437>
- [9] Amirtharaj, J., Mariappan, M. (2023). Exploring the potential uses of Aluminium Metal Matrix Composites (AMMCs) as alternatives to steel bar in Reinforced Concrete (RC) structures-A state of art review. *Journal of Building Engineering*, 80: 108085. <https://doi.org/10.1016/j.jobe.2023.108085>
- [10] Wang, Y.L., Monetta, T. (2023). Systematic study of preparation technology, microstructure characteristics and mechanical behaviors for SiC particle-reinforced metal matrix composites. *Journal of Materials Research and Technology*, 25: 7470-7497. <https://doi.org/10.1016/j.jmrt.2023.07.145>
- [11] MirHashemi, S.M., Amadeh, A., Khodabakhshi, F. (2021). Effects of SiC nanoparticles on the dissimilar friction stir weldability of low-density polyethylene (LDPE) and AA7075 aluminum alloy. *Journal of Materials Research and Technology*, 13: 449-462. <https://doi.org/10.1016/j.jmrt.2021.04.094>
- [12] Donthamsetty, S., Babu, P.S. (2021). An ANN approach for predicting the wear behavior of nano SiC-reinforced A356 MMNCs synthesized by ultrasonic-assisted cavitation. In *Intelligent Manufacturing and Energy Sustainability: Proceedings of ICIMES 2020*, Hyderabad, India, pp. 113-124. [https://doi.org/10.1007/978-981-33-4443-3\\_12](https://doi.org/10.1007/978-981-33-4443-3_12)
- [13] Balasubramanian, I., Maheswaran, R. (2015). Effect of inclusion of SiC particulates on the mechanical resistance behaviour of stir-cast AA6063/SiC composites. *Materials & Design* (1980-2015), 65: 511-520. <https://doi.org/10.1016/j.matdes.2014.09.067>
- [14] Liao, J.H., Yang, L.X., Chen, Z.F., Guan, T.R., Liu, T.L. (2022). Evolution of microstructure and mechanical properties of Cf/SiC-Al composites after high-temperature oxidation. *Materials Characterization*, 194: 112487. <https://doi.org/10.1016/j.matchar.2022.112487>
- [15] Hasan, L.M., Ali, A.M. (2023). Assessment of eggshell and CaCO<sub>3</sub> reinforced recycled aluminium green metal matrix. *Journal of Achievements in Materials and Manufacturing Engineering*, 118(2): 57-61. <http://doi.org/10.5604/01.3001.0053.7662>
- [16] Basavarajappa, K., Jakanur, M., Faheem, M., Baig, M.A.A., Rao, K.S. (2023). Evaluation of properties of Zirconium dioxide reinforced AA7075 composites fabricated via stir casting. In *AIP Conference Proceedings*, Hyderabad, India, 2477(1): 23-24. <https://doi.org/10.1063/5.0125476>



- [17] You, X.H., Xing, Z.Q., Jiang, S.W., Zhu, Y., Lin, Y.H., Qiu, H.S., Nie, R.J., Yang, J.H., Hui, D., Chen, W., Chen, Y. (2024). A review of research on aluminum alloy materials in structural engineering. *Developments in the Built Environment*, 17: 100319. <https://doi.org/10.1016/j.dibe.2023.100319>
- [18] Zhang, Q., Zhu, Y.M., Gao, X., Wu, Y.X., Hutchinson, C. (2020). Training high-strength aluminum alloys to withstand fatigue. *Nature Communications*, 11(1): 5198. <https://doi.org/10.1038/s41467-020-19071-7>
- [19] Mazlan, S., Yidris, N., Koloor, S.S.R., Petrů, M. (2020). Experimental and numerical analysis of fatigue life of aluminum Al 2024-T351 at elevated temperature. *Metals*, 10(12): 1581. <https://doi.org/10.3390/met10121581>
- [20] Almazova, L.A., Sedova, O.S. (2024). Numerical estimation of fatigue life of aluminum alloy specimen with surface defects based on stress-life approach. *Materials Physics and Mechanics*, 52(1): 69-80. [http://doi.org/10.18149/MPM.5212024\\_7](http://doi.org/10.18149/MPM.5212024_7)
- [21] Ibraheem, B., Salman, S.F., Ali, A.H. (2022). Numerical analysis of fatigue life and strength of AA5052 aluminum alloy reinforced with ZrO<sub>2</sub>, TiO<sub>2</sub> and Al<sub>2</sub>O<sub>3</sub> nanoparticles. *Diyala Journal of Engineering Sciences*, 15(2): 83-93. <https://doi.org/10.24237/djes.2022.15208>
- [22] Pul, M. (2021). Effect of ZrO<sub>2</sub> quantity on mechanical properties of ZrO<sub>2</sub>-reinforced aluminum composites produced by the vacuum infiltration technique. *Revista de Metalurgia*, 57(2): 1-13. <https://doi.org/10.3989/revmetalm.195>
- [23] Daniel, E., Obiukwu, O. (2021). Mechanical and physical properties of silicon carbide, aluminum oxide, and epoxy hybrid composite: An overview. *Global Scientific Journals*, 9(11): 2365-2389.
- [24] ASTM, S. (1997). Test methods and definitions for mechanical testing of steel products. In *Annual book of ASTM standards*. <https://doi.org/10.1520/A0370-11>
- [25] ASTM, E8. (2010). Standard test methods for tension testing of metallic materials. In *Annual book of ASTM standards*. [https://doi.org/10.1520/E0008\\_E0008M-08](https://doi.org/10.1520/E0008_E0008M-08)